

## X-Ray and Infrared Spectral Studies of the Ionic Structure of Trimethoprim†–Sulfamethoxazole‡ 1 : 1 Molecular Complex

Hiroshi Nakai,\* Mamoru Takasuka, and Motoo Shiro

Shionogi Research Laboratories, Shionogi and Co. Ltd., Fukushima-ku, Osaka 553, Japan

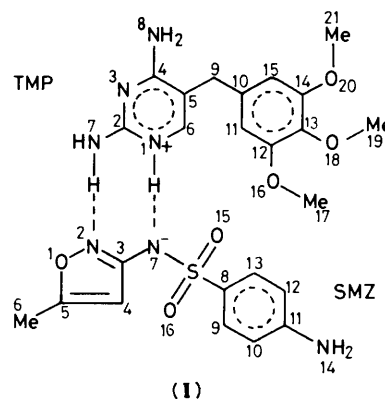
The crystal structure of the title compound (I) has been refined. Those of trimethoprim (TMP) hydrochloride (II) and sulfamethoxazole (SMZ) sodium salt (III) have been determined. In (I) the proton participating in the hydrogen bond between the pyrimidine (TMP) and sulfonamide (SMZ) nitrogen atoms is transferred from SMZ to TMP ( $\geq \text{NH}^+ \cdots \text{N}^- <$ ), with the molecules being ionized. This was verified by comparing the geometrical features exhibited around the nitrogen atoms in (I)–(III). The N–H stretching vibration bands observed in the i.r. ( $3\,500\text{--}2\,500\text{ cm}^{-1}$ ) for (I)–(III) have been assigned taking into consideration the deuterium isotope effects, Raman spectra, and the hydrogen-bonding configuration. The band at  $2\,520\text{ cm}^{-1}$  (broad) in (I) was assigned to a specific  $\text{N}^+\text{--H}$  unit in the hydrogen bond. The ionization of the components in (I) was thus confirmed, contrary to the non-ionic structure previously proposed.

Trimethoprim (TMP) and sulfamethoxazole (SMZ), well known antibacterial substances, are widely used in various combinations. The 1:1 compound precipitated from a solution of the mixture was characterized as a molecular complex.<sup>1</sup> With the mixtures, no injections could be prepared because of the low solubility of the complex formed. It was thus desired to prevent the formation of the complex in aqueous solution.

In order to reveal the nature of the interactions between the components, we have determined the crystal structure of the complex obtained from a benzene solution. Structure (I) consists of a bimolecular unit in which the TMP and SMZ molecules are associated by the hydrogen bonds of  $\text{N}(1)\text{(TMP)} \cdots \text{N}(7)\text{(SMZ)}$  and  $\text{N}(7)\text{(TMP)} \cdots \text{N}(2)\text{(SMZ)}$ . On the difference electron density map, the proton participating in the former hydrogen bond was located closer to  $\text{N}(1)\text{(TMP)}$  ( $1.00\text{ \AA}$ ) than to  $\text{N}(7)\text{(SMZ)}$  ( $1.76\text{ \AA}$ ) to which it was originally bound. Hence, the molecules are ionized to form TMP cations and SMZ anions. This ionization was stereochemically confirmed by comparing the components with the corresponding ions in TMP hydrochloride (II) and SMZ sodium salt (III) and also distinguishing them from the corresponding molecules in the polymorphic form I of TMP<sup>2</sup> (IV) and the form I of SMZ<sup>3</sup> (V).

Giordano *et al.*<sup>1</sup> have reported the i.r. spectrum of (I) in the  $3\,500\text{--}3\,000\text{ cm}^{-1}$  region, but their band assignment was incomplete due to lack of information on the crystal structure at that time. In order to confirm the ionization in (I) by i.r. spectral evidence, we assigned the N–H stretching vibration bands ( $3\,500\text{--}2\,500\text{ cm}^{-1}$ ) for (I)–(III) on the basis of the hydrogen-bonding systems revealed by an X-ray study. The band at  $2\,520\text{ cm}^{-1}$  in (I) (Figure 2) was assigned to  $\text{N}(1)\text{H}^+\text{(TMP)}$  participating in the system  $\text{N}(1)\text{H}^+\text{(TMP)} \cdots \text{N}(7)^-\text{(SMZ)}$ , because it appeared at a lower wavenumber than the band at  $2\,730\text{ cm}^{-1}$  for  $\text{N}(1)\text{H}^+$  in (II) and because it was broad compared with those of polarized hydrogen bonds in crystals. This is direct evidence of ionization occurring in (I).

During our investigation, Giuseppetti *et al.* reported the structure determination of the complex obtained by sublimation of (VI).<sup>4</sup> Its space group and unit-cell parameters agreed well with those of (I) and the crystal structures of (I) and (VI) were essentially the same. However, they stated that the molecules in (VI) were not ionized, based on the position of the proton in



question and the geometrical features exhibited by the components. In other words, the hydrogen bond of  $\text{N}(1)\text{(TMP)} \cdots \text{N}(7)\text{(SMZ)}$  in (VI) was of the type  $\text{N}(1) \cdots \text{HN}(7)$ , in contrast to the polarized one in (I),  $\text{N}(1)\text{H}^+ \cdots \text{N}(7)^-$ . This was very strange in view of the fact that such a polarizable hydrogen bond should be polarized in the same manner when in the same crystal field. Thus, the proton might lie statistically at two independent positions, *i.e.*, delocalization of the proton through the hydrogen bond, and hence, the structure of each component could be a superposition of those of the ionized and neutral molecules. But our i.r. spectral study showed that this was not true for (I). As the i.r. spectrum of (VI) recorded by us was identical with that of (I), the ionic structures of the components in (VI) were established. However, it remained to find the reason why the proton was not uniquely located by the two groups.

Giuseppetti *et al.*<sup>4</sup> suggested that all hydrogen atoms were located geometrically, and then their positions were checked on a difference electron density map. The bond angle of  $\text{C}(2)\text{--N}(1)\text{--C}(6)\text{(TMP)}$  was given as  $117.9^\circ$ . Since the angle was  $115.5^\circ$  in (IV) and  $118^\circ$  in TMP acetate<sup>5</sup> where the nitrogen atom was protonated as in (I), the protonation at  $\text{N}(1)\text{(TMP)}$  could have been expected. The bond length of  $\text{C}(3)\text{--N}(7)\text{(SMZ)}$ ,  $1.367\text{ \AA}$ , was compared with those of  $>\text{C--N}^-$  ( $1.36\text{--}1.37\text{ \AA}$ ) and  $>\text{C--NH}$  ( $1.39\text{--}1.40\text{ \AA}$ ) in the related compounds. This might have suggested deprotonation of  $\text{N}(7)\text{(SMZ)}$ . However, Giuseppetti *et al.* located the proton lying between  $\text{N}(1)\text{(TMP)}$  and  $\text{N}(7)\text{(SMZ)}$  close to  $\text{N}(7)\text{(SMZ)}$ , and not  $\text{N}(1)\text{(TMP)}$ . Perhaps a misreading of the value of the bond angle in the literature for (IV) ( $119.9^\circ$ , instead of  $115.5^\circ$ , in Giuseppetti's

† 2,4-Diamino-5-(3,4,5-trimethoxybenzyl)pyrimidine.

‡ 4-Amino-N-(5-methyl-3-isoxazolyl)benzenesulphonamide.

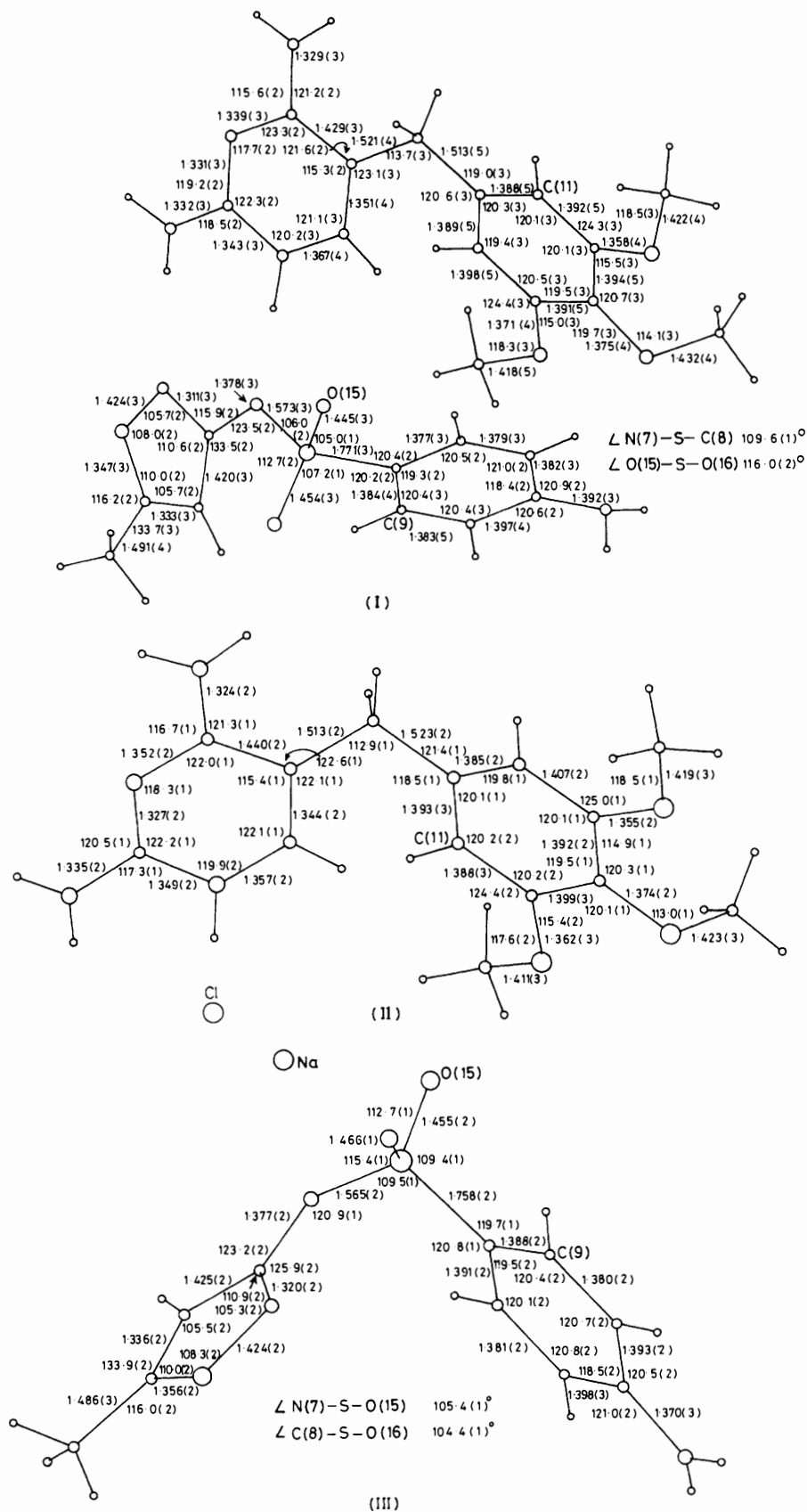
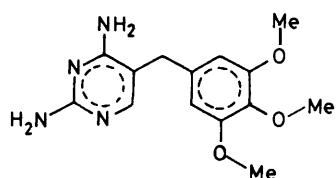


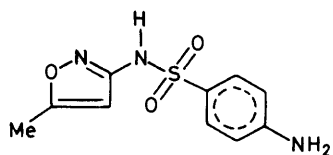
Figure 1. Perspective views of the molecules with bond lengths and angles

**Table 1.** Crystallographic details for (I)—(III)

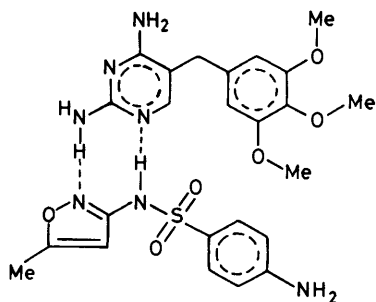
	(I)	(II)	(III)
	$C_{14}H_{19}N_4O_3^+$ , $C_{10}H_{10}N_3O_3S^-$	$C_{14}H_{19}N_4O_3^+, Cl^-$	$C_{10}H_{10}N_3O_3S^-, Na^+$
<i>M</i>	543.6	326.8	275.3
Crystal system	Orthorhombic	Monoclinic	Monoclinic
Space group	<i>Pbca</i>	<i>P2<sub>1</sub>/c</i>	<i>P2<sub>1</sub>/c</i>
<i>a</i> /Å	12.058(2)	22.052(2)	5.908(1)
<i>b</i> /Å	24.479(6)	4.916(1)	17.434(2)
<i>c</i> /Å	17.427(4)	14.256(2)	13.225(2)
$\beta$ /°	90.00	91.39(1)	115.65(1)
<i>U</i> /Å <sup>3</sup>	5 144(2)	1 544.9(2)	1 228.1(3)
<i>Z</i>	8	4	4
<i>D<sub>c</sub></i> /g cm <sup>-3</sup>	1.404	1.405	1.489
Radiation	Mo- <i>K<sub>α</sub></i>	Cu- <i>K<sub>α</sub></i>	Cu- <i>K<sub>α</sub></i>
$\mu$ /cm <sup>-1</sup>	1.8	23.6	26.9
Crystal size/mm	0.12 × 0.25 × 0.25	0.3 × 0.3 × 0.3	0.3 × 0.3 × 0.3
$\theta_{max}$ /°	27.5	70.0	70.0
Number of unique reflections	5 910	2 826	2 280
$\omega$ scan range/°	$\theta < 10$	$\theta < 15$	$\theta < 15$
$\omega$ -2 $\theta$ scan range/°	$\theta \geq 10$	$\theta \geq 15$	$\theta \geq 15$
Scan width parameters <i>A</i> , <i>B</i> , in width = <i>A</i> + <i>B</i> tan $\theta$	1.0, 0.5	1.0, 0.2	1.0, 0.2
Scan speed/° min <sup>-1</sup>	2	2	2



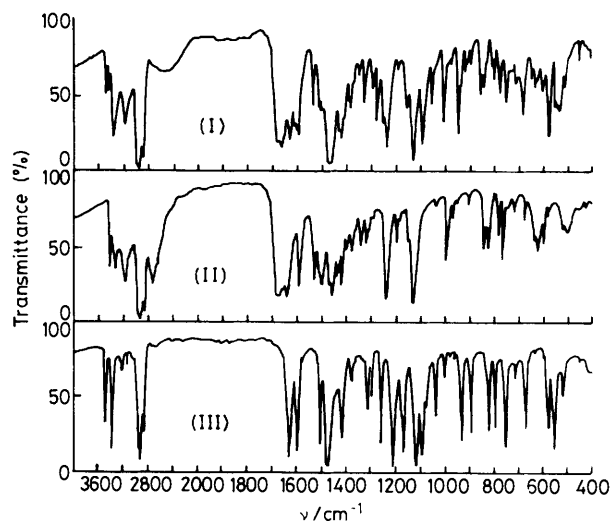
(IV)



(V)



(VI)

**Figure 2.** I.r. spectra of (I)—(III) (Nujol mull)**Experimental**

Crystals of (I) were obtained by sublimation of crystals recrystallized from a benzene solution. Those of (II) and (III) were obtained from water-methanol and aqueous solution, respectively. Deuteriated (I), hereafter indicated by the corresponding number with the suffix D, was prepared by evaporation of acetone- $D_2O$  solution, and (II)<sub>D</sub> and (III)<sub>D</sub> were prepared by evaporation of the respective ethan[ $^2H$ ]ol- $D_2O$  solution. The X-ray powder diffraction patterns were not changed by deuteration.

paper) might account for this. In order to verify the position of the proton by X-ray methods, a new refinement of (I) was undertaken. As a result, the proton was definitely located near N(1)(TMP). Structures (II) and (III) were also determined.

**Crystal Structure Analysis.**—Crystallographic details are listed in Table 1. Three-dimensional intensity data were collected with a Rigaku diffractometer equipped with a pulse-height analyser and a graphite monochromator. Three standard reflections monitored every 100 reflections showed no significant change during data collection. All intensities were

**Table 2.** Hydrogen bonds, X...H-Y, and short contacts around the sodium ion in (III)

<b>(I)</b>			
Symmetry generation			
1	$x, y, z$	5	$-x, -y, -z$
2	$\frac{1}{2} + x, \frac{1}{2} - y, -z$	6	$\frac{1}{2} - x, \frac{1}{2} + y, z$
3	$-x, \frac{1}{2} + y, \frac{1}{2} - z$	7	$x, \frac{1}{2} - y, \frac{1}{2} + z$
4	$\frac{1}{2} - x, -y, \frac{1}{2} + z$	8	$\frac{1}{2} + x, y, \frac{1}{2} - z$
X...H-Y			
N(2)(SMZ)...	N(7)(TMP)[1(0, 0, 0)]	X...Y (Å)	3.015(3)
N(7)(SMZ)...	N(1)(TMP)[1(0, 0, 0)]		2.756(3)
N(14)(SMZ)...	N(8)(TMP)[6(0, -1, 0)]		3.355(3)
O(15)(SMZ)...	N(7)(TMP)[2(-1, 1, 1)]		2.845(3)
O(16)(SMZ)...	N(8)(TMP)[7(0, 1, -1)]		2.932(3)
O(16)(SMZ)...	N(14)(SMZ)[5(0, 1, 1)]		3.150(3)
N(3)(TMP)...	N(14)(SMZ)[6(0, 0, 0)]		3.230(3)
<b>(II)</b>			
Symmetry generation			
1	$x, y, z$	3	$-x, -y, -z$
2	$-x, \frac{1}{2} + y, \frac{1}{2} - z$	4	$x, \frac{1}{2} - y, \frac{1}{2} + z$
X...H-Y			
N(3)...	N(8)[3(2, 1, 1)]	X...Y (Å)	3.063(2)
N(7)...	N(7)[2(2, 0, 1)]		3.373(2)
Cl...	N(1)[1(0, 0, 0)]		3.072(2)
Cl...	N(7)[2(2, -1, 1)]		3.249(2)
Cl...	N(8)[4(0, 0, 0)]		3.223(2)
<b>(III)</b>			
Symmetry generation			
1	$x, y, z$	3	$-x, -y, -z$
2	$-x, \frac{1}{2} + y, \frac{1}{2} - z$	4	$x, \frac{1}{2} - y, \frac{1}{2} + z$
X...H-Y			
O(1)...	N(14)[2(2, -1, 1)]	X...Y (Å)	3.333(2)
O(15)...	N(14)[4(0, 1, 0)]		3.111(2)
O(16)...	N(14)[4(0, 1, 0)]		3.264(2)
Na...X			
Na...	N(2)[1(-1, 0, 0)]		2.413(2)
Na...	N(7)[1(0, 0, 0)]		2.433(2)
Na...	O(15)[1(0, 0, 0)]		2.459(2)
Na...	O(16)[1(-1, 0, 0)]		2.374(1)
Na...	O(16)[3(1, 1, 2)]		2.321(1)

corrected for Lorentz and polarization factors, but not for absorption effects.

**Structure Determination and Refinement.**—The structures were solved by direct methods<sup>6</sup> and improved by block-diagonal least-squares refinement of the positional and the anisotropic thermal parameters of non-hydrogen atoms. Difference electron density maps were then calculated using the low-angle reflections ( $0 < \sin\theta/\lambda \leq 0.36 \text{ \AA}^{-1}$ ), on which all the hydrogen atoms were located. For (I), the positions of the hydrogen atoms were confirmed on a second map similarly calculated with the parameters of the non-hydrogen atoms which were refined using only the high-angle reflections ( $0.55 \leq \sin\theta/\lambda \leq 0.65 \text{ \AA}^{-1}$ ). The positional parameters of all the atoms and the anisotropic thermal parameters of the non-hydrogen atoms were refined by successive least-squares refinement. The temperature factor of each hydrogen atom was assumed to be isotropic and equal to  $B_{\text{eq}} (4/3 \sum_i \beta_{ij} a_i \cdot a_j)$  of the atom to which it was bound.

The function minimized in the refinement was  $\Sigma(w|\Delta F|^2)$ . The weighting scheme was  $w = 1/\sigma^2(F_o)$  for observed reflections with  $|F_o| \geq \sigma(F_o)$  and  $|\Delta F| < 3\sigma(F_o)$ , and  $w = 0$  otherwise.  $\sigma(F_o)$  was

estimated as  $\sigma(F_o) = [\sigma_1^2(F_o) + c^2|F_o|^2]^{1/2}$ , where  $\sigma_1(F_o)$  is the standard deviation due to counting errors.<sup>7</sup> The values of  $c^2$  were respectively 0.000 23, 0.001 24, and 0.000 75 for (I)—(III). The  $R$  values ( $\Sigma|\Delta F|/\Sigma|F_o|$ ) converged to 0.057 (for 3 929 observed reflections with non-zero weight) for (I), 0.030 (2 578) for (II), and 0.027 (2 042) for (III). The atomic scattering factors were calculated using the analytical expression  $f = \Pi(a_i \exp(-b_i \sin^2\theta/\lambda^2)) + c$  ( $i = 1-4$ ).<sup>8</sup> The parameter shifts in the final cycle were less than half the corresponding  $\sigma$  values.

**I.r. and Raman Spectroscopy.**—I.r. spectra of (I)—(III) and (I)<sub>D</sub>—(III)<sub>D</sub> at 25 °C, and those of (I) and (I)<sub>D</sub> at -170 °C were recorded on a JASCO DS-403G grating spectrometer using crystals milled in Nujol oil. The bands at higher wavenumbers (except the C-H stretching vibration band) corresponded well to those for crystals milled in perfluorocarbon. Raman spectra at 25 °C were measured on a JEOL JRS-400T laser Raman spectrophotometer.

## Results and Discussion

**Crystal and Molecular Structures.**—Perspective views of the molecules, with bond lengths and angles involving only non-hydrogen atoms, are shown in Figure 1. Intermolecular hydrogen bonds and short contacts around the sodium ion in (III) are listed in Table 2. Torsion angles necessary to represent the molecular conformations are presented in Table 3.\*

In (I), the bimolecular complex between TMP and SMZ, as shown in Figure 1, seems to be predominantly formed, because the hydrogen bonds of N(1)(TMP)...N(7)(SMZ) (2.756 Å) and N(7)(TMP)...N(2)(SMZ) (3.015 Å) which combine the two molecules are remarkably strong compared with the others in the crystal. The proton participating in the former hydrogen bond is located closer to N(1)(TMP) (1.00 Å) than to N(7)(SMZ) (1.76 Å) to which it is originally bound. Hence, the molecules are ionized to form the TMP cation and the SMZ anion. The value of electron density at the position of the proton calculated by difference Fourier synthesis is  $0.6 e \text{ \AA}^{-3}$ , which is significantly large compared with that of the highest ghost peak,  $0.3 e \text{ \AA}^{-3}$ . Though the peak of the proton tails to N(7)(SMZ), the value at the position 1 Å away from N(7)(SMZ) is less than  $0.2 e \text{ \AA}^{-3}$ .

The protonation of TMP in (II) occurs at N(1), which is confirmed by the formation of the hydrogen bond of N(1)...Cl. In contrast, the atom in (IV) is not protonated through the intermolecular hydrogen bond N(1)...N(7). The bond angles of C(2)—N(1)—C(6) in (II) and (IV) are, respectively, 120.0 and 115.5°. Such enlargement of the bond angle of the pyridine nitrogen atom by protonation is observed in crystals of the zwitterions of cinchomeronic acid and 2-(2-methyl-3-chloroanilino)nicotinic acid.<sup>9</sup> The bond angle in (I), 120.2°, being almost equal to that in (II), verifies the protonation at N(1)(TMP) in (I), *i.e.*, the formation of the TMP cation.

The N(7) atoms of SMZ in (I), (III), and (V) adopt the trigonal configuration. The bonds of N(7)—C(3) and N(7)—S of the anion in (III), deprotonated from N(7), are significantly shorter than the corresponding bonds of the molecule in (V) (Table 3). As this suggested an ionization effect of SMZ on the bonds, the changes in bond energy and  $\pi$ -bond order caused by the ionization were estimated by the CNDO/2 method.<sup>10</sup> Calculations were performed for the molecular and ionic models adopting the same geometry as that of the molecule in

\* Tables of anisotropic thermal parameters, structure factors, and fractional co-ordinates of all the atoms are listed in Supplementary Publication No. SUP 56021 (86 pp.). For details see Instructions for Authors in *J. Chem. Soc., Perkin Trans. 2*, 1984, Issue 1.

**Table 3.** Torsion angles ( $^{\circ}$ ) necessary to represent the molecular conformation. Values in [ ] for SMZ indicate the lengths for the bonds of which the torsion angles are presented.

TMP		(I)	(II)	(IV) <sup>6</sup>
C(4)–C(5)–C(9)–C(10)		–172.9(3)	–156.4(1)	–89.4(1)
C(5)–C(9)–C(10)–C(11)		90.6(4)	62.5(2)	153.3(1)
SMZ		(I)	(III)	(V) <sup>7</sup>
N(2)–C(3)–N(7)–S		171.2(2) [1.378(3)]	8.6(3) [1.377(2)]	–140.8 [1.392(4)]
C(3)–N(7)–S–C(8)		90.4(2) [1.573(3)]	67.8(2) [1.565(2)]	56.7 [1.650(3)]
N(7)–S–C(8)–C(9)		–65.2(3) [1.771(3)]	–144.4(1) [1.758(2)]	–101.5 [1.741(3)]

**Table 4.** I.r. and Raman bands of  $\nu_{\text{NH}}$  and  $\nu_{\text{ND}}$  ( $\text{cm}^{-1}$ ). For Raman bands, wavenumbers and relative intensities are given in parentheses. ( $\sim 0$ ) means unobservable.

(I)		$\nu_{\text{NH}}$		$\nu_{\text{ND}}$		$\nu_{\text{NH}}/\nu_{\text{ND}}$		Assignment
25 $^{\circ}\text{C}$	–170 $^{\circ}\text{C}$	25 $^{\circ}\text{C}$	–170 $^{\circ}\text{C}$	25 $^{\circ}\text{C}$	–170 $^{\circ}\text{C}$	25 $^{\circ}\text{C}$	–170 $^{\circ}\text{C}$	
3 461 ( $\sim 0$ )	3 456	2 599 ( $\sim 0$ )	2 598	1.33	1.33	N(14)H <sub>2</sub> (SMZ) ( $\nu_{\text{as}}$ )		
3 416 ( $\sim 0$ )	3 409	2 553 ( $\sim 0$ )	2 548	1.34	1.34	N(8)H <sub>2</sub> (TMP) ( $\nu_{\text{as}}$ )		
	3 352	2 453 (2 453, 1.5)	2 452		1.37	N(14)H <sub>2</sub> (SMZ) ( $\nu_{\text{s}}$ )		
3 343 (3 350, 3.8)	3 338	2 436 (2 435, 2.3)	2 433		1.37	N(8)H <sub>2</sub> (TMP) ( $\nu_{\text{s}}$ )		
	3 314	2 511 ( $\sim 0$ )	2 502		1.32	N(7)H <sub>2</sub> (TMP) ( $\nu_{\text{as}}$ )		
3 151 (3 143, 1.0)	3 154	2 329 (2 325, 1.0)	2 331	1.35 (1.35)	1.35	N(7)H <sub>2</sub> (TMP) ( $\nu_{\text{s}}$ )		
2 520 ( $\sim 0$ )	2 437	1 918 ( $\sim 0$ )	1 895	1.31	1.29	N(1)H <sup>+</sup> (TMP) ( $\nu$ )		
(II)		$\nu_{\text{ND}}$		$\nu_{\text{NH}}/\nu_{\text{ND}}$		Assignment		
25 $^{\circ}\text{C}$		25 $^{\circ}\text{C}$		25 $^{\circ}\text{C}$				
3 404 (3 409, 0.7)		2 557		1.33		N(7)H <sub>2</sub> ( $\nu_{\text{as}}$ )		
3 318 (3 325, 0.7)		2 505		1.32		N(8)H <sub>2</sub> ( $\nu_{\text{as}}$ )		
3 186sh (3 187, 1.4)		2 391		1.33		N(7)H <sub>2</sub> ( $\nu_{\text{s}}$ )		
3 160 (3 150, 1.0)		2 342		1.35		N(8)H <sub>2</sub> ( $\nu_{\text{s}}$ )		
2 730 (2 745, 0.3)		2 130		1.28		N(1)H <sup>+</sup> ( $\nu$ )		
(III)		$\nu_{\text{ND}}$		$\nu_{\text{NH}}/\nu_{\text{ND}}$		Assignment		
25 $^{\circ}\text{C}$		25 $^{\circ}\text{C}$		25 $^{\circ}\text{C}$				
3 485 (3 489, 0.2)		2 612 ( $\sim 0$ )		1.33		N(14)H <sub>2</sub> ( $\nu_{\text{as}}$ )		
3 376 (3 382, 1.0)		2 454 (2 452, 1.0)		1.38 (1.38)		N(14)H <sub>2</sub> ( $\nu_{\text{s}}$ )		

(V). The bond energies of N(7)–C(3) and N(7)–S are respectively  $-1.159$  and  $-0.922$  in a.u. for the molecular model, and  $-1.246$  and  $-1.014$  for the ionic model. Their  $\pi$ -bond orders are respectively  $0.257$  and  $0.192$  for the former, and  $0.346$  and  $0.276$  for the latter. Hence, the bonds seem to be shortened with increasing  $\pi$ -bond order due to the ionization. The twists about N(7)–S in (III) and (V), represented by the torsion angles of C(3)–N(7)–S–C(8), are very similar and thus the bond shortening of N(7)–S occurring in (III) can be attributed only to the effect of the ionization proved by the present calculation, excluding the effect of the twist about the bond. The bond length in (III) is very close to those of the double bonds of N=S in the region  $1.494$ – $1.580$  Å.<sup>11</sup> The fact that those in (I) and (III) are comparable confirms the existence of the SMZ anion in (I) as well as in (III). For N(7)–C(3), the bond shortening occurring in (I) and (III) may be ascribed to both the effects of the ionization and the twist about the bond. The tendency of bond lengthening in S–O(15), S–O(16), and S–C(8) due to the ionization is supported by the results of the calculation.

Giuseppetti *et al.* used only 1 464 of *ca.* 3 700 independent reflections obtainable in the region of  $\theta \leq 60^\circ$  for Cu- $K_\alpha$  radiation, which meant that the reflection data used contained a relatively large number of lower-angle reflections subject to a contribution from the hydrogen atoms. Under such conditions, N(1)(TMP) would shift, by the least-squares method, close to the position of the proton attached to N(1)(TMP) where no hydrogen atom was located by Giuseppetti *et al.* Hence, the bond angle of C(2)–N(1)–C(6)(TMP),  $117.9(3-6)^\circ$ , is significantly smaller than that in (I) [ $120.2(3)^\circ$ ]. However, its value might approach that in (I) after correction of the shift of N(1)(TMP). The bond lengths of N(7)–C(3)(SMZ) and N(7)–S(SMZ), respectively  $1.367(4-7)$  and  $1.586(4-7)$  Å, agree well with the corresponding ones in (I) [ $1.378(3)$  and  $1.573(3)$  Å], and disagree with those in (V) [ $1.392(4)$  and  $1.650(3)$  Å]. Therefore, the structural features of the components exhibited in Giuseppetti's crystal are common with those of the ions in (I).

*I.r. and Raman Spectroscopy.*—I.r. spectra of (I)–(III) at  $25^\circ\text{C}$  are shown in Figure 2. The band assignments for the N–H and N–D stretching vibrations ( $\nu_{\text{NH}}$  and  $\nu_{\text{ND}}$ ) in the spectra of (I)–(III) and (I)<sub>D</sub>–(III)<sub>D</sub>, as shown in Table 4, were performed by taking into consideration the deuterium isotope effects, the relative intensities of the corresponding Raman bands, and the hydrogen-bond configuration elucidated by the present X-ray study. The spectrum of (I) showed only five of the seven possible bands for  $\nu_{\text{NH}}$ , but all the bands were displayed at  $-170^\circ\text{C}$ . Hence, the spectra of (I) and (I)<sub>D</sub> at  $-170^\circ\text{C}$  were used for the band assignments.

$\nu_{\text{NH}}$  Bands for amino groups in the solid state are usually observed in the  $3\,500$ – $3\,050$   $\text{cm}^{-1}$  region and  $\nu_{\text{ND}}$  bands in the  $2\,600$ – $2\,300$   $\text{cm}^{-1}$  one.<sup>12</sup> For each amino group, the bands in the antisymmetric ( $\nu_{\text{as}}$ ) and symmetric ( $\nu_{\text{s}}$ ) vibration modes appear at higher and lower wavenumbers, respectively. Relative Raman band intensities of  $\nu_{\text{s}}$  bands are stronger than those of  $\nu_{\text{as}}$  bands.<sup>13</sup> Thus, the bands other than those at the lowest wavenumber in (I), (I)<sub>D</sub>, (II), and (II)<sub>D</sub> were allotted to the respective amino groups, based on the criterion that the  $\nu_{\text{NH}}$  and  $\nu_{\text{ND}}$  bands of the amino group engaged in the more intense hydrogen bond appear at the lower wavenumbers. The band at  $2\,730$   $\text{cm}^{-1}$  in (II) was consequently assigned to N(1)H<sup>+</sup> forming the hydrogen bond of N(1)H<sup>+</sup>...Cl<sup>-</sup>. The relationship between the  $\nu_{\text{NH}}$  frequency and the hydrogen bond distance previously derived<sup>14</sup> can be applied to this case. The band at  $2\,437$   $\text{cm}^{-1}$  in (I) may be assigned by analogy to N(1)H<sup>+</sup>(TMP) or N(7)H(SMZ) according to the position of the proton participating in the hydrogen bond formed between N(1) and N(7). However, the band was unequivocally attributed

to N(1)H<sup>+</sup>(TMP) because of its breadth and its appearance at a lower wavenumber than the band for N(1)H<sup>+</sup> in (II). The polarization of the hydrogen bond of N(1)(TMP)...N(7)(SMZ) was thus confirmed. The bands at  $1\,895$  (I)<sub>D</sub> and  $2\,130$  (II)<sub>D</sub>  $\text{cm}^{-1}$  were respectively assigned to the  $\nu_{\text{ND}}$  bands corresponding to the  $\nu_{\text{NH}}$  bands in (I) and (II).

The values of the isotopical frequency ratio ( $\rho = \nu_{\text{NH}}/\nu_{\text{ND}}$ ) for all the  $\nu_{\text{NH}}$  bands in Table 4 are in the region  $1.37$ – $1.28$ . For the amino groups, the  $\rho$  values for the  $\nu_{\text{s}}$  bands are not smaller than the corresponding ones for the  $\nu_{\text{as}}$  bands. These facts establish the present band assignments.

For pyrazinium, pyridinium, and imidazolium halogenides, the correlation between  $\rho$  and  $\nu_{\text{NH}}$  frequency was revealed: the value of  $\rho$  decreases along a curve from  $1.31$  to  $1.21$  as the  $\nu_{\text{NH}}$  frequency decreases from  $2\,900$  to  $2\,050$   $\text{cm}^{-1}$ .<sup>15</sup> The point for N(1)H<sup>+</sup>...Cl<sup>-</sup> in (II),  $\rho$   $1.28$  and  $\nu_{\text{NH}}$   $2\,730$   $\text{cm}^{-1}$ , also falls on the curve. The values for N(1)H<sup>+</sup>(TMP)...N(7)<sup>-</sup>(SMZ) in (I), respectively  $1.29$  and  $2\,437$   $\text{cm}^{-1}$ , are similar to the corresponding one for the salts. The hydrogen bond for which each of the value ranges in the region is regarded as a medium-strong one: the barrier separating the two minima of the potential energy function remains relatively high and, hence, the proton stays preferentially in one minimum. For stronger hydrogen bonds having a relatively low potential barrier, the  $\rho$  values are considered to be close to unity as in the case of O–H...O hydrogen bonds.<sup>15</sup> Therefore, it is unlikely that the hydrogen bond of N(1)(TMP)...N(7)(SMZ) in (I) would be so strong that the proton would be delocalized through the bond as proposed in the Introduction.

## References

- 1 F. Giordano, G. P. Bettinetti, A. La Manna, and P. Ferloni, *Farmaco, Ed. Sci.*, 1977, **32**, 889.
- 2 T. F. Koetzle and G. J. B. Williams, *J. Am. Chem. Soc.*, 1976, **98**, 2074.
- 3 J. Rambaud, R. Roques, S. Alberola, and F. Sabon, *Bull. Soc. Chim. Fr.*, 1980, 56.
- 4 G. Giuseppetti, C. Tadini, G. P. Bettinetti, F. Giordano, and A. La Manna, *Farmaco, Ed. Sci.*, 1980, **35**, 138.
- 5 R. C. Haltiwanger, M. Sc. Thesis, University of Virginia, Charlottesville, 1971.
- 6 P. Main, S. E. Hull, L. Lessinger, G. Germain, J. P. Declercq, and M. M. Woolfson, 'MULTAN78: A System of Computer Programs for the Automatic Solution of Crystal Structures from X-ray Diffraction Data,' Universities of York and Louvain.
- 7 D. F. Grant, R. C. G. Killean, and J. L. Lawrence, *Acta Crystallogr.*, 1969, **B25**, 374.
- 8 'International Tables for X-Ray Crystallography,' Kynoch Press, Birmingham, 1974, vol. IV.
- 9 (a) F. Takusagawa, K. Hirotsu, and A. Shimada, *Bull. Chem. Soc. Jpn.*, 1973, **46**, 2669; (b) M. Takasuka, H. Nakai, and M. Shiro, *J. Chem. Soc., Perkin Trans. 2*, 1982, 1061.
- 10 J. A. Pople and D. L. Beveridge, 'Approximate Molecular Orbital Theory,' McGraw-Hill, New York, 1970.
- 11 F. Iwasaki, *Kagaku No Ryoiki*, 1979, **33**, 59.
- 12 (a) L. J. Bellamy, 'Advances in Infrared Group Frequencies,' Methuen, London, 1968; (b) R. N. Jones and C. Sandorfy in W. West, 'Chemical Applications of Spectroscopy,' Interscience, New York, 1956, ch. 4.
- 13 (a) G. Herzberg, 'Molecular Spectra and Molecular Structure,' 'Infrared and Raman Spectra of Polyatomic Molecules,' Van Nostrand, New York, 1945; (b) E. B. Wilson, jun., J. C. Decius, and P. C. Cross, 'Molecular Vibrations,' McGraw-Hill, New York, 1955.
- 14 (a) K. Nakamoto, M. Margoshes, and R. E. Rundle, *J. Am. Chem. Soc.*, 1955, **77**, 6480; (b) R. Schroeder and E. R. Lippincott, *J. Phys. Chem.*, 1957, **61**, 921.
- 15 A. Novak, *Struct. Bonding (Berlin)*, 1974, **18**, 177.